Solid-Fluid Interaction Analysis in Fixed Mesh

and its Application to Functional Design of Component

*Yuta Tamura[1], Atsushi Kawaguchi[2], Toru Hamasaki[2], *Shigenobu Okazawa[1] and Satoyuki Tanaka[2]

[1]Department of Transportation and Environmental System, Graduate School of Engineering,
Hiroshima University, Higashi-Hiroshima 739-8527, Japan
[2]Toyota Central R & D Labs, 41-1 Yokomichi, Nagakute, Aichi 480-1192, Japan

*okazawa@hiroshima-u.ac.jp

Abstract

This paper describes computational method with finite element method in fixed mesh for flexible solid-fluid interaction problems. Finite element method in fixed mesh can treat large deformation without mesh failure and contact between different materials. This paper describes governing equation in strong form with mixture theory and capturing method of free-moving material interfaces. In addition, after verification of the above computational method in simple example, we apply the proposed procedure to practical solid-fluid interaction behavior such as functional design of component.

Keywords: Solid-Fluid Interaction, Fixed Mesh, Functional Design

Introduction

Recent years, high performance computing is developed dramatically. Various simulations can be performed by the high performance computing. A dynamics phenomenon has few phenomena to occur by the motion of single solid and fluid. There is more solid-fluid interaction phenomenon. Therefore, not only solid analysis and fluid analysis, but also solid-fluid interaction analysis is essential. Various studies have been performed about solid-fluid interaction analysis. The present approach establishes one governing equation for both solid and fluid models using mixture theory assuming incompressibility in the full Eulerian framework. Hyperelasticity for solid and Newtonian fluid are employed in the constitutive equations. A discretization of the proposed formulation for solid-fluid interaction dynamics is based on an explicit finite element method. The explicit finite element method reduces computational cost, except that the finite different method instead of the finite element method is used to solve Poisson and advective equations.

In this study, we focus on solid-fluid interaction analysis for automotive rubber bush. In the analyses, the strain velocity affects the stiffness. It is one of a characteristic of rubber bush so-called the velocity dependence. Our final goal is to simulate the rubber bush considering the mechanical characteristic.

Mixture government equations

The present formulation treats interaction problem of shaft, rubber and viscous fluid for the rubber bush analysis. Fig. 1 is a representative volume with solid and fluid. In the Eulerian formulation, the one computational mesh contains different plural materials. In this section, we formulate the Eulerian mixture governing equations using volume fraction (Drew and Passman 1998).
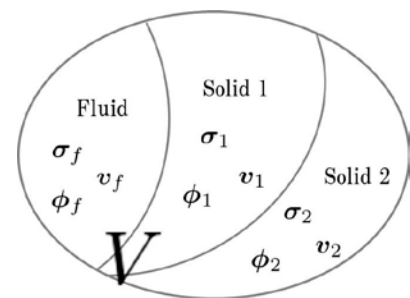
Figure 1. Representative volume with solid and fluid

1

For the following discussion, the subscripts *1*, *2* and *f* indicate quantities of solid1, solid2 and fluid respectively. The equations of motion for three materials are as follows,

$$\rho_1\left(\frac{\partial \boldsymbol{v}_1}{\partial t} + (\boldsymbol{v}_1 \cdot \nabla)\boldsymbol{v}_1\right) = \nabla \cdot \boldsymbol{\sigma}_1 + \rho_1 \boldsymbol{b} \tag{1}$$

$$\rho_2\left(\frac{\partial \boldsymbol{v}_2}{\partial t} + (\boldsymbol{v}_2 \cdot \nabla)\boldsymbol{v}_2\right) = \nabla \cdot \boldsymbol{\sigma}_2 + \rho_2 \boldsymbol{b} \tag{2}$$

$$\rho_f\left(\frac{\partial \boldsymbol{v}_f}{\partial t} + (\boldsymbol{v}_f \cdot \nabla)\boldsymbol{v}_f\right) = \nabla \cdot \boldsymbol{\sigma}_f + \rho_f \boldsymbol{b} \tag{3}$$

Where ρ is density, $\boldsymbol{v}$ is velocity and σ is Cauchy stress. We assume that body force $\boldsymbol{b}$ is identical for volume. The equations of continuity for incompressibility are as follow,

$$\nabla \cdot \boldsymbol{v}_1 = 0 \tag{4}$$

$$\nabla \cdot \boldsymbol{v}_2 = 0 \tag{5}$$

$$\nabla \cdot \boldsymbol{v}_f = 0 \tag{6}$$

We make the equation of motion and continuity volume average. The mixture equation of motion and continuity are as follow,

$$\rho_{mix}\left(\frac{\partial \boldsymbol{v}_{mix}}{\partial t} + (\boldsymbol{v}_{mix} \cdot \nabla)\boldsymbol{v}_{mix}\right) = \nabla \cdot \boldsymbol{\sigma}_{mix} + \rho_{mix}\boldsymbol{b} \tag{7}$$

$$\nabla \cdot \boldsymbol{v}_{mix} = 0 \tag{8}$$

The index mix is meant mixture, and mixture physical quantity is satisfied with follow equation.

$$\boldsymbol{v}_{mix} = \phi_1 \boldsymbol{v}_1 + \phi_2 \boldsymbol{v}_2 + \phi_3 \boldsymbol{v}_3 \tag{9}$$

$$\rho_{mix} = \phi_1 \rho_1 + \phi_2 \rho_2 + \phi_3 \rho_3 \tag{10}$$

$$\boldsymbol{\sigma}_{mix} = \phi_1 \boldsymbol{\sigma}_1 + \phi_2 \boldsymbol{\sigma}_2 + \phi_3 \boldsymbol{\sigma}_3 \tag{11}$$

ϕ_i is volume rate function of materials. Total of volume rate function are always 1 shown in the following.

$$\phi_1 + \phi_2 + \phi_3 = 1 \tag{12}$$

By solving the mixture equation, it is possible to be analyzed a unified way without solving to discriminate equations for each material.

Computational flow

The mixture stress σ_{mix} in Eq. (7) is divided into deviatoric stress and pressure. Where I is the second order unit tensor.

$$\boldsymbol{\sigma}_{mix} = \boldsymbol{\sigma}_1' - p_{mix}\boldsymbol{I} \tag{13}$$

The mixture deviatoric stress σ'_{mix} is evaluated with respective volume fractions. On the other hand, the mixture pressure p_{mix} can be calculated with SMAC method. The following subsections review computational flow. For details, see references (Okazawa, Terasawa, Kurumatani, Terada and Kashiyama, 2010; Okazawa, Kashiyama and Kaneko, 2007; Benson and Okazawa, 2004).

Intermediate velocity

We discretize spatially the mixture governing Eq. (7) by finite element method without advection term (Chorin, 1980). The present study employs 8-node isoparametric element for 3-dimensional analysis. For numerical integration, we use selective reduced integration to avoid volumetric locking. The explicit method with the central difference method is used to advance time. The discretized equation is as follows

$$\boldsymbol{v}^* = \boldsymbol{v} + \Delta t \boldsymbol{M}^{-1}\left(\boldsymbol{F}_{ext} - \boldsymbol{F}_{int}\right) \tag{14}$$

$\boldsymbol{M}$ is mass matrix, $\boldsymbol{v}$ is velocity vector at current time and $\boldsymbol{v}^*$ is intermediate velocity vector. $\boldsymbol{F}_{int}$ is internal force and $\boldsymbol{F}_{ext}$ is external force. We adopt the lumped mass matrix. Δt is time increment.

Pressure and Modification of Velocity

After calculating pressure with conventional SMAC method, the intermediate velocity is modified (A. Amsden and F. Harlow, 2007). The corrective pressure is calculated in center of all computational mesh. By using the corrective pressure, we modify velocity to satisfy Eq. (8).

Advective calculation and interface capturing

Because the above calculation for the intermediate velocity excludes advective term, we advect the physical quantities with the 1st order upwind difference method. The advected quantities are velocity and left Cauchy-Green deformation tensor. Also regarding accurate mass advection, we employ PLIC (Piecewise Linear Interface Calculation) method (D.L. Youngs, 1982; Rider, and Kothe 1998). The PLIC method linear approximate to the interface of the mesh from the volume rate as Fig. 2. We calculate a volume flux using the interfacial information like Fig. 3. By using the PLIC method, it is possible to capture of free-moving material interfaces.
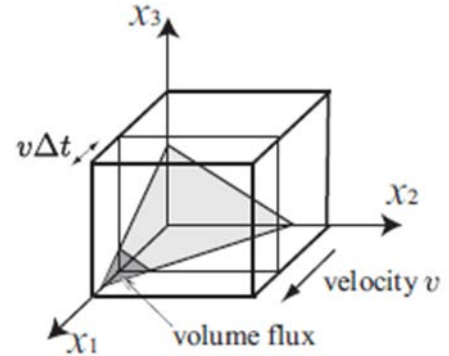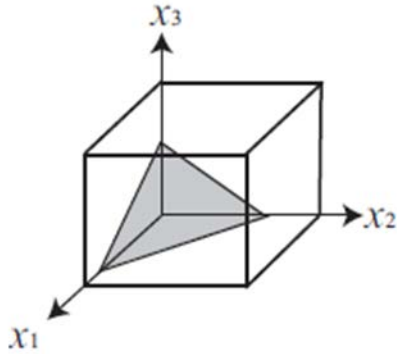
Figure 2. Material interface in PLIC method   **Figure 3. Volume flux with PLIC method**

Numerical simulation

We apply the described Eulerian formulation using mixture theory to rubber bush analysis. Fig. 4, Fig. 5 is computational models. We treat three materials, shaft, rubber and viscous fluid. As for computational model 2, the duct of fluid is narrow. Therefore, the influence of fluid becomes strong. We give a frequency 200Hz~400Hz and a displacement ±5mm to the shaft. The shaft is rigid body. We calculate the internal force of x-direction component of the rubber and fluid part.
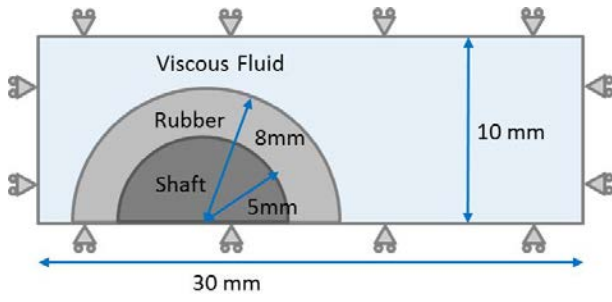
Figure 4. Computational model 1
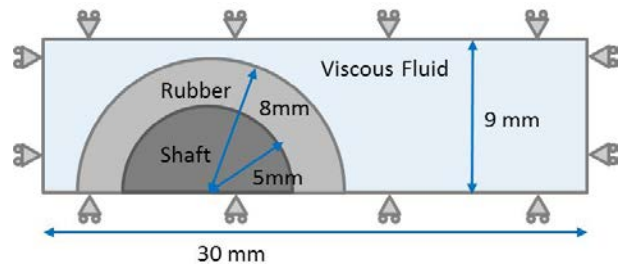
Figure 5. Computational model 2
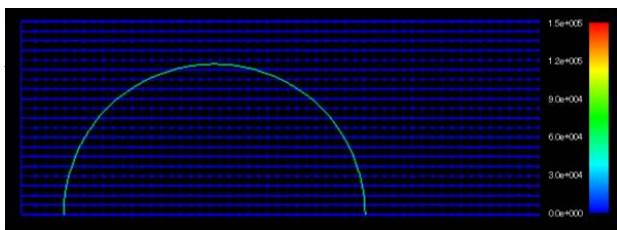
t=0.0 (model1)
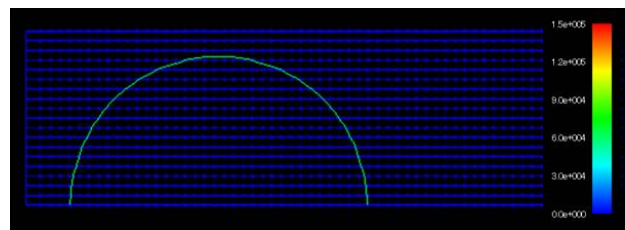
t=0.0 (model2)
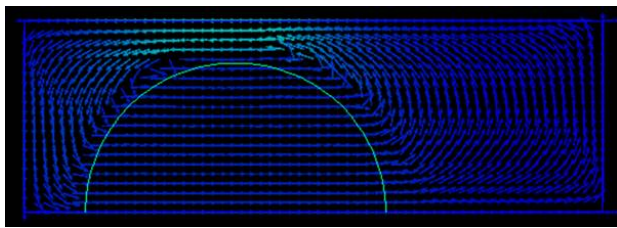
t=0.025 (model1)
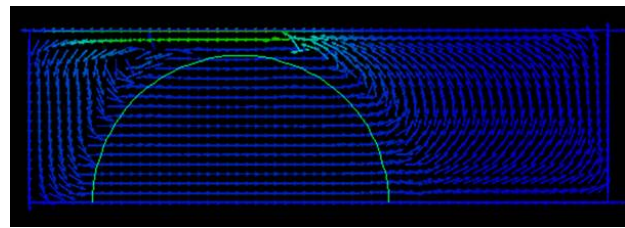
t=0.025 (model2)
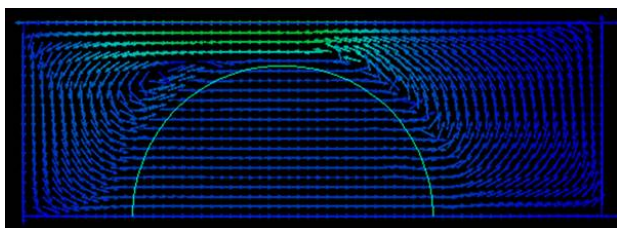
t=0.05 (model1)
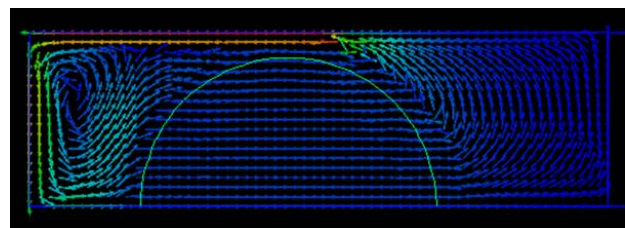
t=0.025 (model2)
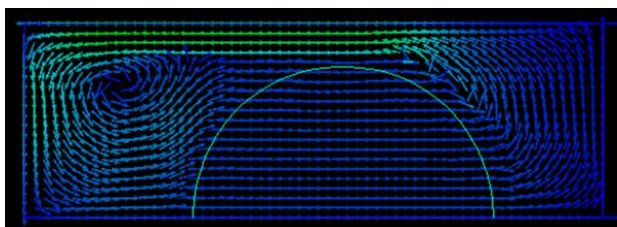
t=0.075 (model1)
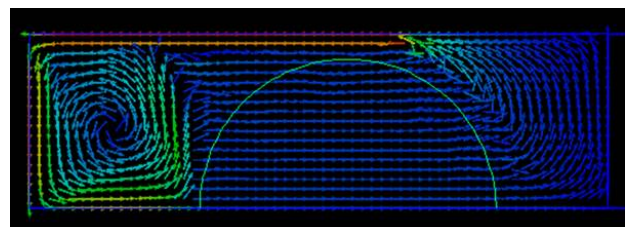
t=0.075 (model2)

Figure 6. Velocity line of each model

4

Table 1. Material Parameters

	Shaft	Rubber	Fluid
Young's Modulus (MPa)	300	300	-
Poisson Ration (-)	0.5	0.5	-
Density (10^{-6} kg/mm^3)	5.0	1.0	0.5
Viscosity (10^{-3} Pa・s)	-	-	7.7

Fig.6 shows velocity line. We confirm that velocity line changes with solid movement. We compare the result of analysis computational model 1 and computational model 2. In computational model 2, the duct of fluid is narrow. Flow velocity of computational model 2 is faster than computational model 1. Therefore, it is thought that the influence of fluid is strong with computational model 2.

Computational model 1   **Computational model 2**
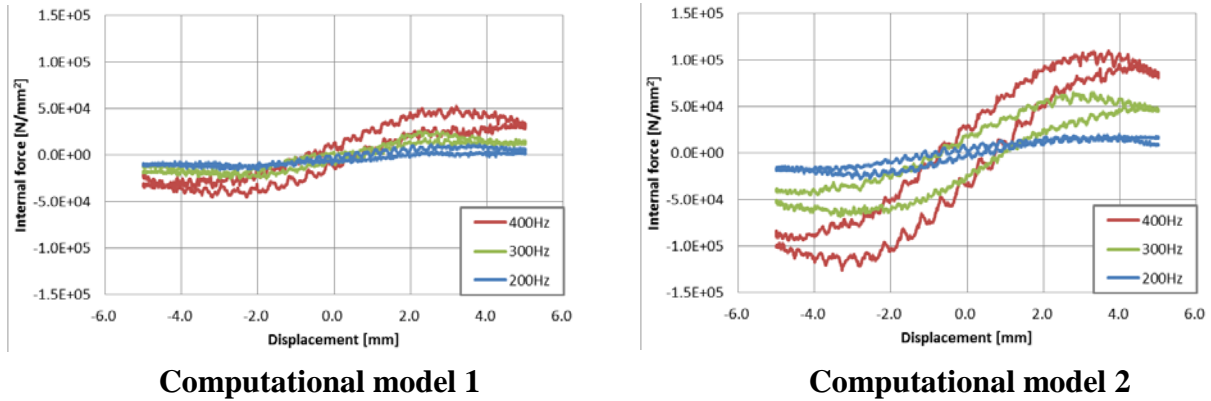
Figure 7. Internal force of rubber and viscous fluid

Fig.7 shows the internal force of rubber and viscous fluid. We confirm that the gradient of graph is increasing both computational model 1 and computational model 2. In addition, the path of graph is different in the forward and return. The graph of computational model 2 is the large oval. Therefore, we think that viscous fluid is affects the path of graph.

Next, we perform a parameter identification of stiffness coefficient 'K' and damping coefficient 'C' using a least squares method. The equations of approximation are as follows,

$$F = Kx + Cv \qquad\qquad (15)$$

Where x is displacement of the shaft and v is applied velocity.
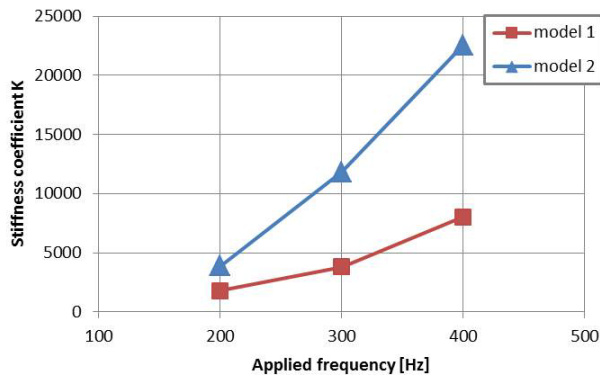
Figure 8. Stiffness coefficient 'K'   **Figure 9. Damping coefficient 'C'**
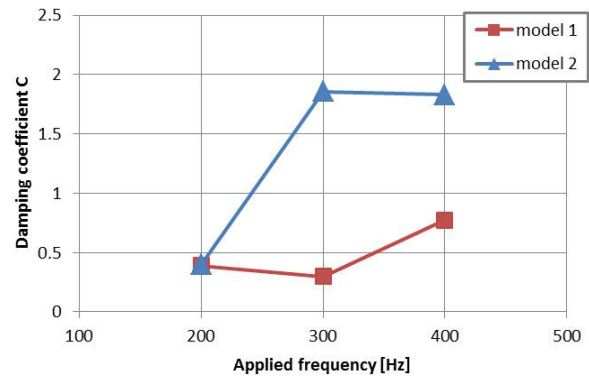
We confirm that the stiffness coefficient 'K' has increased by the vibration frequency. The computational model 2 indicates a large value. The stiffness coefficient 'K' depends on the gradient of graph of Fig.7. Fig.9 shows the damping coefficient 'C'. The computational model 2 indicates a larger value than the computational model 1. The computational model 2 is strongly influenced by the viscous fluid. Therefore, we consider the damping coefficient 'C' is larger in the computational model 2. As a result, the stiffness coefficient is dependent on the gradient of graph of Fig.7. The damping coefficient is dependent on the area of graph of Fig.7.

Conclusions

The present paper have described the mixture Eulerian formulation and the vibration simulation of the automotive rubber bush. We performed a parameter identification of stiffness coefficient 'K' and damping coefficient 'C' using a least squares method. The future study, we improve the computational model. We apply the digital data such as voxel data to the computational model. Therefore, it is possible to simulate the rubber bush analysis with high accuracy.

References

D.A. Drew and S.L. Passman (1998), Theory of Multicomponent Fluids, *Springer*.

S. Okazawa, H. Terasawa, M. Kurumatani, K. Terada and K. Kashiyama (2010), Eulerian finite cover method for solid dynamics, *International Journal of Computational Methods*, **7**, pp.33-54.

S. Okazawa, K. Kashiyama and Y. Kaneko (2007), Eulerian formulation using stabilized finite element method for large deformation solid dynamics, *International Journal for Numerical Methods in Engineering*, **72**, pp.1544-1559.

D.J. Benson and S. Okazawa (2004), Contact in a multi-material Eulerian finite element formulation, *Computer Methods in Applied Mechanics and Engineering*, **193**, pp.4277-4295.

A. Amsden and F. Harlow (2007), The SMAC method: *A numerical technique for calculating incompressible fluid flows*, Technical Report LA-4370 , Los Alamos National Laboratory , pp.1286-1305.

A.J Chorin (1980), Flame advection and propagation algorithm, *Journal of Computational Physics*, 35, pp.1-31

D.L. Youngs (1982) , Time-dependent multi-material flow with large fluid distortion, in K.W. Morton and M.J. Baines (eds), *Numerical Methods for Fluid Dynamics*, , Academic, New York, pp.273-285.

W.j. Rider, and D.B. Kothe (1998), Reconstructing volume tracking, *Journal of Computational Physics*, 114, pp.112-152.